

Focus on the Likely: Test-time Instance-based Uncertainty Removal

Johannes Schneider University of Liechtenstein Liechtenstein
johannes.schneider@uni.li

Abstract

We ask: Does focusing on classes predicted as likely improve model predictions? We aim for an affirmative answer by proposing two novel test-time fine-tuning methods to improve uncertain model predictions. Instead of greedily selecting the most likely class, we introduce an additional step, *focus on the likely classes*, to refine predictions. By applying a theoretically motivated single gradient descent step with a large learning rate, we refine predictions when an initial forward pass indicates high uncertainty. This aligns predictions more closely with the ideal of assigning zero probability to less plausible outcomes. The experimental evaluation demonstrates accuracy gains for one of our methods, which emphasizes shared features among likely classes, across diverse text and image domain models.

1 Introduction

State-of-the-art optimization methods in supervised and self-supervised learning, prevalent across subdisciplines ranging from image recognition in computer vision to text generation with large language models, typically minimize cross-entropy loss. The optimization objective aligns with the ideal scenario where a model assigns probability one to the correct class and zero to all others, achieving perfect class discrimination. Such outcomes are achievable on training data since neural networks can memorize even random data Zhang et al. [2021]. However, during test-time, a model might exhibit (as we also show) uncertainty, particularly in cases where it errs. Nevertheless, current decoding strategies still greedily select the most likely class, even when uncertain. In this work, we proclaim that before making a choice in cases of high uncertainty, one should reflect on the estimated class distribution and narrow down the options by focusing on the most likely classes through fine-tuning of the network. That is, we aim to further contrast likely and unlikely outcomes through optimization, aiming to eliminate all unlikely choices from consideration. The high-level idea is illustrated in Figure 1.

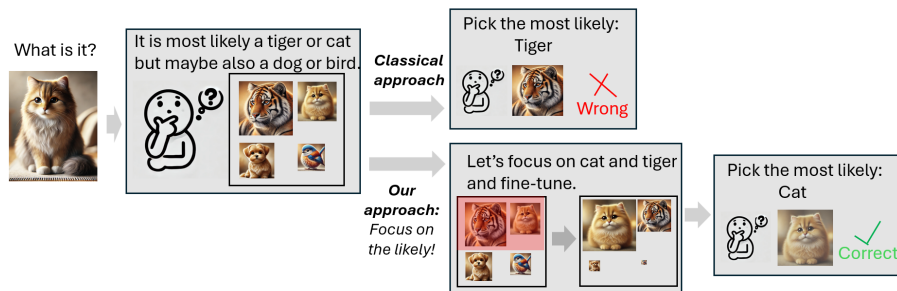


Figure 1: High level idea: Fine-Tune based on likely initial classes.

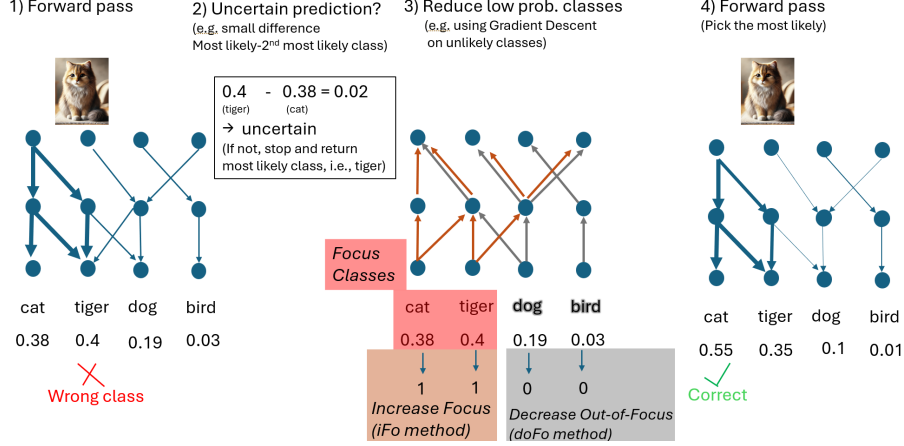


Figure 2: Our test-time approaches (iFo/doFo): If a prediction exhibits high uncertainty, changes are done to focus on likely (focus) classes either by increasing focus classes or decreasing all others.

More technically, a network ideally should assign zero probability to choices considered unlikely. To achieve this, we introduce an *additional step focusing on likely classes during the prediction process if the initial forward pass yields high uncertainty*, as illustrated in the overview in Figure 2. We apply gradient descent at test-time in two distinct ways, either by *Decreasing outputs of Out-of-Focus (doFo)* towards 0 or by *Increasing outputs for Focus classes (iFo)*. While both methods aim at the same goal, i.e., focus on the likely, they follow different rationales, e.g., amplifying or lowering shared features among different sets of classes. It is not clear that these methods yield gains. Thus, the fundamental research question becomes: *Does focusing on classes predicted as likely improve model predictions?*

As the naive optimization method is computationally very expensive due to the need to conduct potentially 10s or more forward and backward passes per sample, we employ an uncertainty assessment step to limit our method to cases, where it likely helps, and furthermore only perform a single extra forward and backward pass per sample, which due to the nature of the problem (as we discuss) yields often better outcomes as performing many iterations. We evaluate our methods across multiple datasets and classifiers on text generation and image recognition tasks. We demonstrate that iFo, which relies on enhancing shared features among likely classes, improves prediction accuracy in most cases, whereas doFo, which suppresses features of unlikely classes, produces more mixed results.

2 Methodology

Next, we describe how we aim to improve predictions for high-uncertainty cases at test-time, as outlined in Figure 2. We add two components to the classical (single-forward) prediction process: (i) An *uncertainty assessment* procedure which decides whether to apply the focus optimization or not; (ii) A *focus optimization* module, which alters predictions.

Uncertainty Assessment: The prediction uncertainty assessment determines whether focus optimization should be applied to a specific sample or not. Focus optimization introduces overhead that should be avoided if it is unlikely to result in meaningful changes, particularly when uncertainty is low. Furthermore, the lower the uncertainty, the higher the risk that modifying the prediction introduces errors. We quantify uncertainty based on how strongly a classifier favors the predicted class compared to other classes. Specifically, we measure the uncertainty as the difference between the probabilities of the most likely and second-most likely classes. If this difference is large, the prediction is intuitively likely correct, as alternative classes have significantly lower probabilities. Concretely, we consider a model f , such as a neural network, that outputs logit values $f_c(X)$ for each class $c \in C$. The softmax layer converts the logit values $f_c(X)$ into probability estimates $p_c(X)$. Let $m(i)$ denote the class with the i -th highest probability for input X ; thus, $p_{m(1)}(X)$ and $p_{m(2)}(X)$ represent the highest and second-highest probabilities, respectively. We define the difference as:

$$\Delta_{1,2} = p_{m(1)}(X) - p_{m(2)}(X) \quad (1)$$

Algorithm 1 Focus on the Likely: iFo and doFo

Require: $f(\cdot|\theta)$: Model with parameters θ ; X : input; mode $\in \{\text{iFo}, \text{doFo}\}$; T : Iterations (default: 1)
1: n_f : Number of focus classes (default: 2); $d_{1,2}$: uncertainty threshold (default: 0.04)
2: η : learning rate (default: 1.6e-5(iFo), 2.56e-4(doFo))
3: **// Step 1: Uncertainty Assessment**
4: Compute logits $f(X) = [f_c(X)]_{c \in C}$ and probabilities $p_c(X) = \frac{e^{f_c(X)}}{\sum_{k \in C} e^{f_k(X)}}$
5: Sort probabilities so that $p_{m(1)}(X) \geq p_{m(2)}(X) \geq \dots$
6: Compute $\Delta_{1,2} = p_{m(1)}(X) - p_{m(2)}(X)$ {Eq. (1)}
7: **if** $\Delta_{1,2} \geq d_{1,2}$ **then** return **end if** {If model is confident return without optimization}
8: **// Step 2: Focus Optimization**
9: $F := \{m(i) | i \in [1, n_f]\}$ {Focus classes}
10: **for** $t = 1$ to T **do**
11: $\theta \leftarrow \theta - \eta \nabla_{\theta} L_{\text{mode}}(X)$ {Eq. (2) using focus classes F }
12: **end for**

When $\Delta_{1,2}$ is large, the model f is quite certain that the most likely class is correct. Hence, focus optimization is unlikely to improve. Thus, we apply our optimization technique for a sample X if $\Delta_{1,2} < d_{1,2}$ for a user-given threshold $d_{1,2}$.

Focus Optimization: We employ gradient descent for a fixed number of iterations, i.e., just one except for one experiment, to increase focus on the most likely classes, called “focus classes” $F \subset C$, where C is the set of all classes. We discuss two seemingly opposing methods illustrated in Figure 2: i) *Decreasing outputs of Out-of-FOcus classes* $C \setminus F$ (doFo) and ii) *Increasing outputs of FOCus classes* F (iFo). While both methods share the same goal, they employ different rationales: iFo amplifies features shared among focus classes F , provided these features positively contribute to their likelihood. The underlying *assumption* is that if a feature positively contributes to the most likely predictions, it is likely highly relevant. This approach is motivated by the belief that features shared among multiple classes are generally more robust. In contrast, doFo suppresses features shared between focus and out-of-focus classes. The underlying *assumption* here is that features relevant to less likely classes are probably less important. This relies on the idea that these classes have accumulated significantly less probability mass, making their associated features potentially less credible. Visually, in the center panel of Figure 2, iFo increases activations of the subnetworks indicated by beige arrows, whereas doFo decreases those indicated by grey arrows. It is unclear whether either of these methods provides benefits. As we will demonstrate, improvements from doFo are inconsistent across tasks, while iFo performs more reliably. We set $|F| \geq 2$, meaning we focus on at least the two most likely classes for each sample X . Additionally, we apply gradient descent directly to the raw logits f_c rather than to probabilities p_c , as indicated in Algorithm 1. When optimizing the log outputs $\log(p_c)$ from a softmax layer—typical in classical cross-entropy loss optimization—we must account for the normalization inherent in softmax. This results in a conceptual overlap of our approaches, simultaneously increasing focus-class probabilities and decreasing out-of-focus class probabilities, as discussed in the appendix. For iFo, we maximize the logits—and consequently the probabilities—of the focus classes F . For doFo, we minimize the logits of the out-of-focus classes $C \setminus F$. Thus, we minimize the following losses:

$$L_{\text{iFo}}(X) = -\frac{\sum_{c \in F} f_c(X)}{|F|}, \quad L_{\text{doFo}}(x) = \frac{\sum_{c \in (C \setminus F)} f_c(X)}{|C \setminus F|} \quad (2)$$

These loss functions are among the simplest expressing our idea. The division to get a per-class average loss makes the learning rate less sensitive to the number of focus classes $|F|$.

3 Theoretical Motivation

We provide intuition by relating our method—optimizing multiple classes F —to the scenario of optimizing toward a single class, as is common in typical cross-entropy loss computations. Using a simple model and gradient descent equations, we examine which features become more relevant, distinguishing between those shared among classes and those unique to specific classes. We also

discuss why a single-step optimization with a larger learning rate can be more stable for iFo compared to multi-step optimization with a smaller learning rate.

Model: We use a simple case with three output classes $C = \{y_0, y_1, y_2\}$ and focus classes $F = \{y_0, y_1\}$. To compute the final output y_i being logits we employ four input features $X = \{x_0, x_1, x_2, x_3\}$. The input features x_j originate from a prior layer l , i.e., $x_j = l(a_j, c'_k) = l(z_i)$ with activations a_j and parameters c'_k . We assume that the optimization process has yielded some parameters c_i , which define our network f . Outputs $y_i := f_i(X)$ are computed as: $y_0 = c_0x_0 + c_4x_3$, $y_1 = c_1x_1 + c_5x_3$, $y_2 = c_2x_2 + c_6x_3$. We assume that a feature value cannot be negative, i.e., $x_i \geq 0$, which occurs, for example, after activations pass through a non-linearity like *ReLU*. We consider updates to parameters c_i based on the loss from our methods: iFo with $L_{iFo} = -(y_0 + y_1)$, doFo with $L_{doFo} = y_2$ (Eq. 2), and from optimizing just a single class either $L_{y_i,+} = y_i$ or $L_{y_i,-} = -y_i$. In short, $L_{y_i,\pm} = \pm y_i$. We investigate updates to parameters c_i due to backpropagation: $c_i \leftarrow c_i - \eta \frac{\partial L}{\partial c_i}$ with $L \in \{L_{iFo}, L_{doFo}, L_{y_i,\pm}\}$.

Analysis: Partial derivatives with respect to prior layer outputs z_i (More details in Appendix):

$$\frac{\partial L_{y_j,\pm}}{\partial z_i} = \pm(c_j \frac{\partial x_j}{\partial z_i} + c_{4+j} \frac{\partial x_3}{\partial z_i}), \quad \frac{\partial L_{iFo}}{\partial z_i} = -c_0 \frac{\partial x_0}{\partial z_i} - c_1 \frac{\partial x_1}{\partial z_i} - (c_4 + c_5) \frac{\partial x_3}{\partial z_i}, \quad \frac{\partial L_{doFo}}{\partial z_i} = c_2 \frac{\partial x_2}{\partial z_i} + c_6 \frac{\partial x_3}{\partial z_i} \quad (3)$$

We compare the updates for loss L_{iFo} using the focus classes y_0 and y_1 against using just either y_0 or y_1 , i.e., the loss $L_{y_0,-}$ or $L_{y_1,-}$. Wlog., we use $L_{y_0,-}$. The changes related to parameters c_0, c_1 tied exclusively to the feature x_0 , indicative of class y_0 , are identical. That is the change of either of the them is of the same magnitude, e.g., $\frac{\partial L_{iFo}}{\partial c_0} = \frac{\partial L_{y_0,-}}{\partial c_0} = x_0$. However, the behavior for the shared feature x_3 differs between iFo and single class optimization. The feature’s impact on outputs can disproportionately grow or diminish: Assume both c_4 and c_5 have the same sign, i.e., $c_4 > 0, c_5 > 0$. Then $\frac{\partial L_{iFo}}{\partial z_i} > \frac{\partial L_{y_0,-}}{\partial z_i}$ as $c_4 + c_5 > c_4$. In turn, the change to the shared feature x_3 is larger. Thus, in the subsequent update, both c_4 and c_5 experience stronger changes compared to single-class optimization, since $\frac{\partial L_{iFo}}{\partial c_i} = x_3$ for $i \in \{4, 5\}$. That is, there is a “double growth effect”, where the growth of x_3 amplifies the growth of parameters c_4 and c_5 , and vice-versa. This can lead to instability in an iterative process, e.g., the shared features becomes the sole decision criteria with exploding coefficients. This effect is not present if we perform just a single step (with large learning rate). However, in both single-step and multi-step optimization, we observe that for iFo the shared feature undergoes more extreme alterations compared to class-specific features, potentially leading to over-reliance on that feature. On the one hand relying more on shared features seems flawed as class-specific features that matter only for one of the (focus) classes also play a role in discriminating them. However, the fact that we have high uncertainty and we know that the classifier deemed both classes y_0 and y_1 relevant, hints that the shared features should play a bigger role than class-specific features as the classifier overall assigns more probability mass to classes due to them than compared to class-specific features. If both c_4, c_5 have different signs, i.e., the changes to x_3 are less for iFo than for optimizing only y_0 and in turn also c_4, c_5 change less, meaning that the relevance of x_3 to the decision process diminishes relative to single class optimization.

An analogous analysis applies to doFo, leading, in summary, to the following: iFo tends to amplify features shared among focus classes F (if their presence positively contributes to likelihood), whereas doFo tends to suppress features shared between focus and out-of-focus classes.

4 Experiments

Setup. We evaluate our methods on multiple standard vision and language tasks and models (references in Appendix). For image classification, we use ImageNet, CalTech-256 (Cal256), CIFAR-100 (Ci100), and (balanced) EMNIST. We trained VGG-13(V13), ResNet-18(R18), and MobileNetV3-13 (M13) for image classification on Ci100, Cal256 and EMNIST. For ImageNet we used pre-trained models from PyTorch’s torchvision, namely Efficient-Net B0/B7 (EffB0/EffB7), ResNet-50 (R50), ConvNext-Base (CoNetB), MobileNet-V3 large (MOBV3), VGG-16 BN (VGG16). The image datasets are diverse covering natural images in color as well as black and white handwriting. Furthermore, they also vary in size and resolution.

For language modeling, we use from HuggingFace: GPT-2 (124MB version), Llama 3.2 1B, QWEN 2.5 1.5B, and Gemma-2 2B. We evaluate on OpenWebText (an open-source replication of the

WebText dataset from OpenAI), SimpleWiki (Wikipedia articles written in simple English), and legal contracts. Our datasets cover output classes ranging from about 50 to more than 50000 to ensure generalizability. For hyperparameters, if not otherwise stated, we use defaults specified in Algorithm 1. Regarding the optimizer, we chose not to use Adam, as it relies on moments that anticipate "future" or non-local changes—effectively hinting at how parameter updates might evolve when moving in a certain direction across iterations. Two properties of our method make this less relevant. First, we chose to use fixed focus classes for a single sample X throughout the optimization. Second, we use mostly just a single step for stability and computational reasons. Thus, we expect limited variation in the optimization direction across iterations and, in turn, anticipating upcoming iterations provides little benefit. Following similar reasoning, we set momentum to 0, since momentum primarily prevents zig-zagging and escaping local minima by averaging gradients across multiple batches and iterations. We also set weight decay to 0, as weight decay penalizes large weights, causing the network to rely on many features. However, our philosophy is the opposite: We aim to focus on fewer relevant classes and features. Therefore, weight decay might counteract our method.

Measures and Notation. We compare the model f_{Opt} resulting from our optimization (Algorithm 1) against the original, unmodified model f serving as baseline. We consider various configurations $O = \{F, D\} = O_{Img} \cup O_{Text}$, meaning pairs of models and datasets (f, D) for images O_{Img} and text O_{Text} . To compute measures of variation for O_{Text} , we considered 10k predictions as one unit for which measures are computed. We report measures for individual configurations $(f, D) \in O$ and a test dataset $D_{te} = \{X, Y\} \subset D$ and aggregated measured on configurations O . The subset $D_{te,1,2} \subset D_{te}$ are the uncertain samples, where optimization takes place, i.e., $D_{te,1,2} = |\{(x, y) \in D_{te} | \Delta_{1,2} < d_{1,2}\}|$. The correctly classified samples of model f' are $co(f') = |\{\arg \max_c f'_c(x) = y | (x, y) \in D_{te,1,2}\}|$. $\Delta_{Corr} := co(f_{Opt}) - co(f)$ refers to the gain, i.e., the difference of the number of correct samples of f and f_{Opt} . $\overline{\Delta_{Corr}}$ is the average Δ_{Corr} across a set of configurations. $\#\Delta_{Corr>0} := \{(\Delta_{Corr} > 0) | (f, D) \in O'\}$ refers to the number of configurations in O' , where our method increases the number of correct samples, i.e., where $\Delta_{Corr} > 0$. Δ_{Acc} refers to the change in accuracy due to the application of our method for the samples we applied our method, e.g., $\Delta_{Acc} = \frac{\overline{\Delta_{Corr}}}{|D_{te,1,2}|}$. The fraction of samples for which optimization took place is $\frac{|D_{te,1,2}|}{|D|}$.

Uncertainty Assessment. *Experiment 1 - Top-k Accuracy vs. Threshold $d_{1,2}$:* First, we assess implicit assumptions that make our method more or less likely to be beneficial. We investigate the impact of our uncertainty assessment on the top-k accuracy, i.e., a network's output is correct as long as the correct class is among the k most likely classes. We want that even in case of high uncertainty (i.e., when keeping only samples with small differences $d_{1,2}$) the top-k accuracy rapidly increases for k . The top-2 accuracy should be significantly higher than the top-1 accuracy and the top-1 accuracy should be low. If the top-1 accuracy is 0 and top-2 accuracy is 1 then our method can only improve predictions with two focus classes $n_f = |F| = 2$. We compute the top-k accuracy on datasets $D_{te,1,2}$ using multiple uncertainty levels, i.e., very high ($d_{1,2} = 0.01$), high ($d_{1,2} = 0.1$) and very low ($d_{1,2} = 1$), i.e. using all data.

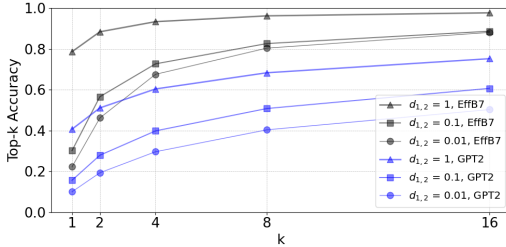


Figure 3: Top-k Accuracy for GPT2 on OpenWeb-Text and EffB7 on ImageNet

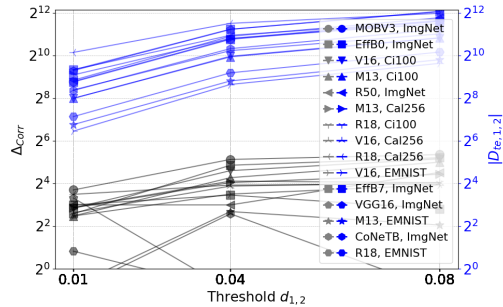


Figure 4: Relation between number of predictions $|D_{te,1,2}|$ and gain in terms in correct predictions Δ_{Corr} due to iFo for image recognition

Result: In Figure 3 (more in Appendix) we observe that for higher uncertainty (i.e., smaller $d_{1,2}$) the top-k likelihood also gets smaller, i.e., the correct class is less likely among the top-k correct classes, while it grows with k for all uncertainty levels $d_{1,2}$. The plot hints that applying our method only on

high uncertainty samples (small $d_{1,2}$) is favorable in multiple ways: First, the chances that changes to models lead to an incorrect prediction are lower, as the odds of the most likely class being incorrect before applying our method are already high. Second, the top-1 accuracy is lower and the change from top-1 to top-2 is larger than for low uncertainty. Third, we do not need to change probabilities a lot. This seems an easier, more local optimization task, e.g., for an iterative process we likely need fewer iterations, meaning also less computation.

For GPT2 the curves for all uncertainty levels are significantly flatter than for EffB7 on image data. Flatter curves indicate that fixing a prediction is harder as there are more candidate classes with a comparable likelihood. However, the top-1 accuracy for GPT2 is also lower, meaning that changing the prediction is likely not harmful (as the most likely class is probably already wrong). Thus, overall, on the outset it is not clear, for which model and dataset combination our method should perform best. However, both models seem reasonable candidates to test our method, as they fulfill the basic criteria that top-2 accuracy is significantly higher than top-1, while top-1 accuracy is not very high for low certainty.

Hyperparameters. *Experiment 2 - Uncertainty threshold $d_{1,2}$:* We assess our method by varying the uncertainty threshold $d_{1,2}$ for O_{Img} . To this end, we show the difference in terms of the absolute number of correct samples (Δ_{Corr}) between the unmodified baseline model f and the tuned model f_{Opt} . We also show the number of samples $|D_{te,1,2}|$ below the uncertainty threshold. We used default settings but started with a learning rate of $\eta = 0.001$.¹

Results: Figure 4 for iFo (Plot for doFo in Appendix) shows that generally allowing for larger differences $d_{1,2}$ leads to more corrected samples Δ_{Corr} – at least up to some point. The outcome is non-obvious as one the one hand, larger differences $d_{1,2}$ imply that more samples might be fixed (e.g., larger $|D_{te,1,2}|$). On the other hand, changing samples with less uncertainty is more risky as the top-1 accuracy is more likely correct, potentially leading to more errors. Furthermore, the growth of Δ_{Corr} is mostly slower than that of $|D_{te,1,2}|$ meaning that the efficiency of our method decreases with larger thresholds, i.e., we must optimize more and more samples to obtain an additional correct sample with larger $d_{1,2}$. The behavior, especially for larger thresholds, is volatile across configurations. For some datasets and classifiers Δ_{Corr} grows monotonously with $d_{1,2}$, while for others it grows only up to some point before decreasing and potentially even being negative. Note, that we used the same learning rate for all configurations O_{Img} . This is one reason why for some models only few samples got changed, which also makes results more noisy for individual models. Therefore, we included many configurations. Overall, there is no clearly optimal choice for $d_{1,2}$ for all configurations. We decided to use $d_{1,2} = 0.04$ as default choice as lower thresholds tend to lead to only very few samples in the test data $D_{te,1,2}$.

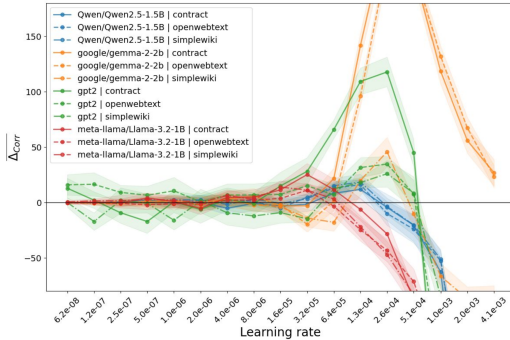


Figure 5: Δ_{Corr} using different learning rates for iFo for each configuration O_{Text} with shaded areas being $1/3$ Std

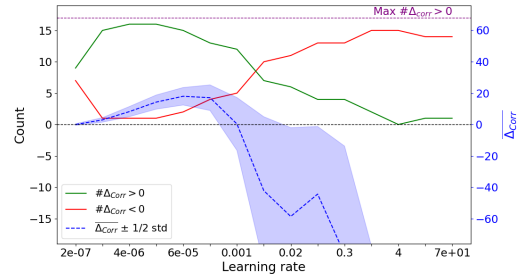


Figure 6: Average Δ_{Corr} and $\#\Delta_{Corr} > 0$ for different learning rates for iFo for all configurations O_{Img}

Experiment 3 - Iterations T (single vs. many): Our algorithm 1 relies on the learning rate η and the number of optimization iterations T . For computational reasons we would like to minimize iterations and we might even hope for better outcomes if doing so as elaborated in Section 3 – at least for high learning rates. Thus, we investigate if performing a single step with a large learning rate, leads to similar gains Δ_{Corr} as conducting many steps with a small learning rate. Generally, large learning rates can lead to instability and hamper convergence, while small ones might lead to getting stuck

¹The behavior is qualitatively similar for other learning rates.

in local optima. For multiple iterations, we chose three learning rates of $\eta \in \{0.01, 0.001, 1e-5\}$ and conduct $T = 8$ iterations. $\eta = 0.01$ is a (too) high learning rate, while the other two are close to the default learning rates we employ for iFo and doFo, respectively for O_{Img} . We compare the multi-step performance against doing just a single step with learning rate $\eta' = \eta \cdot 2^{Power}$ for $Power \in \{0, 1, 2, 3\}$. As measure, we use the relative difference of correct samples for single step $\Delta_{Corr, Si}$ and multi-step $\Delta_{Corr, Mu}$ by showing a scatter plot with individual performance data points combined with a violin-plot indicating the distribution for all configurations O_{Img} .

Results: The plots 7 for iFo (and 9 for doFo in Appendix) indicate that single step optimization overall is mostly on par or better than multi-step. After the first parameter updates (Iteration 0), both are identical. Then, the differences slightly grow with the number of iterations but they tend to be rather small for doFo, i.e., less than 25%. For iFo, we frequently observe that multi-step iterations cause deteriorating performance (for large learning rates), e.g., at iteration 8 the violin plot shows a considerable probability mass at 1, indicating that single step performance $\Delta_{Corr, Si}$ is much better – aligned with our theoretical reasoning in Section 3. The fact that we can employ a single-step with a large learning rate is also a consequence from having just a single sample. When fine-tuning with many diverse samples in a batch, gradients are likely to change more during training as inputs and targets vary between batches. Our method tend to alter the same (focus) classes F in each iteration using the same sample X with the same targets. In fact, one might even assume that gradients are approximately keeping their direction though potentially changing in magnitude as one gets closer to the optimum.

Experiment 4 - Learning rate η : The learning rate is a highly relevant choice when fine-tuning a neural network. The literature recommends different learning rates per layer (e.g., freezing lower layers) and choosing learning rates also depending on the network size. We opted for a simple approach that aims at finding just two (separate) learning rates - one for iFo and one for doFo for all configurations O_{Img} , while we chose network dependent learning rates for O_{Text} . We emphasize that this is a stringent requirement as most vision models were originally trained with different learning rates. We report for how many of our configurations O_{Img} our method is indeed beneficial, i.e., count $\#\Delta_{Corr} > 0$ and those where it is harmful ($\#\Delta_{Corr} < 0$). We also show the average difference of correct samples between the unmodified and optimized model, i.e., $\overline{\Delta_{Corr}}$ and half its standard deviation.

Results: Figures 5 and 6 for iFo (and 11, 13 for doFo in Appendix) show that for small learning rates neither significant gains nor losses are observed, while for large learning rates the outcomes for our methods deteriorate. This aligns with conventional wisdom for classical cross-entropy loss optimization of a single class though not necessarily obvious as we always also optimize towards the most likely class of the baseline. However, the larger the learning rate the more likely our algorithm can overcome large differences in (initial) predictions and turn a correct prediction into a wrong prediction. Inbetween we find that both the average benefit ($\overline{\Delta_{Corr}}$) as well as the number of configurations with $\Delta_{Corr} > 0$ increase with the learning rate up to some point. When looking at aggregates (Figure 6) the point of change is different for both metrics, i.e., the average benefit has a maximum for larger learning rates than the number of configurations. This is intuitive, as each (model, dataset) configuration has a different maximum learning rate before its outcomes deteriorate - often dramatically as visible in Figure 5 showing individual text configurations. As such, we opted for a rather small learning rate of $1.6e-05$ for iFo and a larger one of 0.000256 for doFo for our vision models. For text, we choose a network dependent learning rate (but the same rate for all datasets), which maximizes Δ_{Corr} according to Figure 5. Note, there is a rather large range of learning rates that lead to gains on all three datasets for each model.

Experiment 5 - Overall Performance (for fixed hyperparameters): Table 1 shows key metrics for iFo for O_{Img} when using default hyperparameters stated in Algorithm 1, while Figure 5 shows individual configurations O_{Text} for varying learning rates also indicating that there exists a learning rate for each model yielding gains on all datasets (in Appendix we have Table 3 for iFo with fixed learning rate on text and Tables for doFo). Overall, we observe mostly gains for iFo – sometimes considerable gains, but the magnitude varies considerably. For doFo results are mixed with overall gains being marginal at best, which we elaborate on in the discussion section. Note that only a limited number of samples exhibit high decision uncertainty. In particular, for simple datasets like EMNIST our method is applied to less than 1% all samples (i.e., $\frac{|D_{te, 12}|}{D_{te}}$ is small). While for hard datasets, i.e., Cal256 which contains many classes but few training samples, leading to lower performing models, the application rate is much higher. The hardness of the datasets is also shown by the accuracy of the

Table 1: Performance for iFo with the same hyperparameters across all configurations O_{Img}

Dataset	Model	$\frac{ D_{te,1,2} }{ D }$	$ D_{te,1,2} $	Acc.f		Δ_{Acc}
				Baseline	Ours, iFo	
Cal25	M13	17.7	1773	8.66	9.39	0.73
Cal25	R18	30.2	3015	12.97	13.57	0.6
Cal25	V16	11.8	1182	7.97	9.21	1.24
Ci100	M13	4.9	980	19.65	22.2	2.55
Ci100	R18	10.1	2015	22.87	24.04	1.17
Ci100	V16	5.0	994	18.88	22.33	3.45
EMNIS	M13	0.5	383	41.36	41.62	0.26
EMNIS	R18	0.3	270	40.04	41.03	0.99
EMNIS	V16	0.4	305	37.62	40.46	2.84
ImgNe	CoNeTB	2.6	1282	30.11	30.73	0.62
ImgNe	EffB0	4.8	2403	27.01	28.67	1.66
ImgNe	EffB7	3.4	1718	22.93	23.51	0.58
ImgNe	MOBV3	3.5	1770	24.46	26.21	1.75
ImgNe	R50	3.8	1893	27.26	27.95	0.69
ImgNe	VGG16	4.8	2385	23.44	23.27	-0.17

unmodified model on the uncertain samples. But there is also significant variance of $|D_{te,12}|$ due to architecture. That is, for a fixed dataset, the number of samples investigated varies by network. There is no clear indication that better performing models (on a given dataset) exhibit less uncertain samples, also there is no consistent behavior for the same architecture across different datasets. Δ_{Acc} also shows no strong patterns. Thus, suggesting that the iFo method seems rather general.

Further experiments and analysis covering combining our method with test-time tuning on inputs and applying XAI can be found in the appendix.

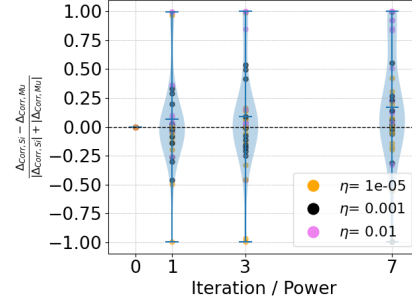
5 Related Work

Decoding strategy: Historically, the class associated with the highest output value was selected. However, with the emergence of generative models, various decoding strategies have been developed. In particular, sampling from the output distribution while excluding unlikely outcomes (e.g., using top-p, also known as nucleus sampling in LLMs [Holtzman et al., 2019]) has become common. The inventor of nucleus sampling [Holtzman et al., 2019] proposed this technique to address shortcomings in text generation, such as making generated text more engaging. We idealize the notion that outcomes considered inappropriate for sampling should ideally have zero probability.

Test-time training for domain adaptation: Many studies addressing domain adaptation (e.g., Kim et al. [2024], Osowiechi et al. [2024], Karmanov et al. [2024], Sun et al. [2020], Liu et al. [2021], Wang et al. [2023]) assume that test-time data originate from a domain different from that of the training data. Instead of framing our approach in terms of distributions, we assume that an individual sample might not be classified perfectly. Our method also applies when test data are identical to training data. For example, many LLMs fail to perfectly predict training data even after training, a scenario in which our method is naturally beneficial, though the rationale of domain adaptation does not directly apply.

Test-time tuning using data (also) beyond sample: A large class of work requires data additional to the sample to classify and performs classical fine-tuning, e.g., for a sample (X, Y) the model is optimized to predict Y given X or just X in a self-supervised setting. This is in stark contrast, as we only focus on the sample at hand and for a sample X we consider a set of classes F for which we do not know the correct outcome. Commonly, test-time tuning relies on nearest neighbors and conducts a form of local learning by adjusting the model to the chosen data. For example, RNNs [Sun et al., 2024] have been adjusted using local fine-tuning [Bottou and Vapnik, 1992]. Hardt and Sun [2023] fine-tunes on nearest neighbors, while Hübotter et al. [2024] improves nearest neighbor selection. Wang et al. [2023] requires a batch of test samples leveraging feature distributions to create class prototypes using also nearest neighbors. Mummadi et al. [2021] aims at accounting for distribution shifts using the soft likelihood ratio (SLR) loss, i.e., the ordinary likelihood loss weighted by the output probability. This bears similarity with our iFo method, if we employed softmax outputs. However, we use logits and we focus on a small subset F of C . Conceptually, *iFo* and *doFo* are multi-class optimizations, where we consider all focus (and out-of focus) classes as target classes. While we work on raw logits, one might also use alternatives such as quadratic loss [Demirkaya et al.,

Figure 7: Relative change in predictions Δ_{Corr} over iterations compared to single step with learning rate 2^{Iter} for iFo across all configurations O_{Img}



2020] or a mixture of quadratic and cross-entropy loss[Hui et al., 2023] that is even claimed to lead to better calibration. Gupta et al. [2014] showed that during training more confusable class increase empirical loss, suggesting that at test-time this also leads to higher uncertainty between such classes. *Test-time tuning using only samples to classify*: Some studies specifically investigated how to improve models using test data alone, although typically involving multiple samples. Wang et al. [2020] employed entropy minimization, optimizing only channel-wise scaling and shifting instead of all model parameters, in contrast to our approach. Specifically, in contrast to our work, they optimized the network toward a single class ($|F| = 1$), whereas we avoid entropy optimization and instead consider multiple likely classes ($|F| = 2$). Additionally, our method requires only a single sample, rather than a dataset of test samples. Their method demonstrates improvements solely on corrupted data, whereas our approach targets the more common scenario involving non-corrupted data. Sun et al. [2020] and subsequent studies, such as Liu et al. [2021], also utilize single samples but require an auxiliary task trained in a self-supervised manner (e.g., predicting image rotations). In contrast, our method is supervised and reflective—it leverages initial prediction outputs for improvements without needing any auxiliary task. Numerous other studies have explored test-time adaptation (surveyed in Liang et al. [2024]); some require modifications to training, input transformations, estimation of training data characteristics, or various forms of augmentation. Many of these techniques are complementary to our approach and could potentially be integrated to enhance results. Additionally, many works emphasize computational efficiency exclusively (e.g., Karmanov et al. [2024] employing lookups rather than model updates), which is not our primary concern.

6 Limitations, Discussion and Conclusions

This work set out to answer the research question *Does focusing on classes predicted as likely improve model predictions?* by aiming for a positive confirmation proposing two optimization methods. Our theoretical model enables concise statements and offers deeper insights into the proposed methods; however, it lacks general theorems necessary to conclusively answer the research question. Our empirical findings suggest that the assumption that reducing features of unlikely classes is beneficial does not hold consistently, as indicated by the mixed outcomes observed for doFo. This may be due to our hyperparameter choices—specifically, aggressively reducing shared features across all but the two most likely classes. However, our assumption that features belonging to classes with low probabilities are less useful might also be incorrect. It seems more to be the case that non-shared features among (non-likely) classes should be reduced as they might be less robust as the fact that a feature is “shared” provides support for its reliability. Such investigations are left for future work. In contrast, enhancing shared features of likely classes (iFo) proves more beneficial. This yields the conjecture that *reducing reliance on a few strongly activated features is beneficial during regular offline training, whereas enhancing such features can be advantageous at test time*; that is, our findings suggest benefits from reinforcing already prominent features at test-time, while weight decay reducing strong feature reliance during training is helpful. Our feature-level perspective aligns with the contrasting objectives of training phases: broad generalization during offline training and targeted local adaptation during online, test-time training. However, this conjecture deserves systematic study. Furthermore, it is well-known that lower-layer features are more general and robust than those in higher layers, suggesting that our approaches should account for this difference. Our work was also constrained by limited computational resources. We mostly had to forgo hyperparameter tuning, which might have led to better outcomes. Specifically, we did not systematically explore hyperparameters such as the number of focus classes, instead relying on reasonable defaults. We empirically demonstrated, supported by theoretical reasoning, that performing a single gradient step (with high learning rates) can effectively replace multiple gradient computations in our setup. This makes our method more practical, though the computational overhead is still considerable. Additionally, our method uses uncertainty estimates. We leveraged the standard notion of softmax probabilities of neural networks, which are known to be poorly calibrated [Guo et al., 2017]. Applying calibration techniques might further enhance our results.

References

- L. Bottou and V. Vapnik. Local learning algorithms. *Neural computation*, 4(6):888–900, 1992.
- C. Chen et al. Qwen2.5-coder technical report. *arXiv preprint arXiv:2409.12186*, 2024.

- G. Cohen, S. Afshar, J. Tapson, and A. Van Schaik. Emnist: Extending mnist to handwritten letters. In *2017 international joint conference on neural networks (IJCNN)*, pages 2921–2926. IEEE, 2017.
- A. V. del Moral. Legal contracts dataset. https://huggingface.co/datasets/albertvillanova/legal_contracts. Accessed: 2024-12-01.
- A. Demirkaya, J. Chen, and S. Oymak. Exploring the role of loss functions in multiclass classification. In *2020 54th annual conference on information sciences and systems (ciss)*, pages 1–5. IEEE, 2020.
- J. Deng, W. Dong, R. Socher, L.-J. Li, K. Li, and L. Fei-Fei. Imagenet: A large-scale hierarchical image database. In *2009 IEEE conference on computer vision and pattern recognition*, pages 248–255, 2009.
- A. Gokaslan and V. Cohen. Openwebtextcorpus. <http://Skylion007.github.io/OpenWebTextCorpus>. Accessed: 2024-08.
- G. Griffin, A. Holub, and P. Perona. Caltech-256 object category dataset, 2007. URL <https://resolver.caltech.edu/CaltechAUTHORS:CNS-TR-2007-001>.
- C. Guo, G. Pleiss, Y. Sun, and K. Q. Weinberger. On calibration of modern neural networks. In *International conference on machine learning*, pages 1321–1330. PMLR, 2017.
- M. R. Gupta, S. Bengio, and J. Weston. Training highly multiclass classifiers. *The Journal of Machine Learning Research*, 15(1):1461–1492, 2014.
- M. Hardt and Y. Sun. Test-time training on nearest neighbors for large language models. *arXiv preprint arXiv:2305.18466*, 2023.
- K. He, X. Zhang, S. Ren, and J. Sun. Deep residual learning for image recognition. In *Conf. on computer vision and pattern recognition*, 2016.
- A. Holtzman, J. Buys, L. Du, M. Forbes, and Y. Choi. The curious case of neural text degeneration. *arXiv preprint arXiv:1904.09751*, 2019.
- A. Howard, M. Sandler, G. Chu, L.-C. Chen, B. Chen, M. Tan, W. Wang, Y. Zhu, R. Pang, V. Vasudevan, et al. Searching for mobilenetv3. In *Proceedings of the IEEE/CVF international conference on computer vision*, pages 1314–1324, 2019.
- J. Hübötter, S. Bongni, I. Hakimi, and A. Krause. Efficiently learning at test-time: Active fine-tuning of llms. *arXiv preprint arXiv:2410.08020*, 2024.
- L. Hui, M. Belkin, and S. Wright. Cut your losses with squentropy. In *International Conference on Machine Learning*, pages 14114–14131. PMLR, 2023.
- A. Karmanov, D. Guan, S. Lu, A. El Saddik, and E. Xing. Efficient test-time adaptation of vision-language models. In *Proceedings of the IEEE/CVF Conference on Computer Vision and Pattern Recognition*, pages 14162–14171, 2024.
- E. Kim, M. Sun, C. Baek, A. Raghunathan, and J. Z. Kolter. Test-time adaptation induces stronger accuracy and agreement-on-the-line. *Advances in Neural Information Processing Systems*, 37: 120184–120220, 2024.
- A. Krizhevsky and G. Hinton. Learning multiple layers of features from tiny images. Technical report, 2009.
- J. Liang, R. He, and T. Tan. A comprehensive survey on test-time adaptation under distribution shifts. *International Journal of Computer Vision*, pages 1–34, 2024.
- Y. Liu, P. Kothari, B. Van Delft, B. Bellot-Gurlet, T. Mordan, and A. Alahi. Ttt++: When does self-supervised test-time training fail or thrive? *Advances in Neural Information Processing Systems*, 34:21808–21820, 2021.

- A. Madaan, N. Tandon, P. Gupta, S. Hallinan, L. Gao, S. Wiegrefe, U. Alon, N. Dziri, S. Prabhunoye, Y. Yang, et al. Self-refine: Iterative refinement with self-feedback. *Advances in Neural Information Processing Systems*, 36, 2024.
- C. K. Mummadi, R. Hutmacher, K. Rambach, E. Levinkov, T. Brox, and J. H. Metzen. Test-time adaptation to distribution shift by confidence maximization and input transformation. *arXiv preprint arXiv:2106.14999*, 2021.
- D. Osowiechi, G. A. V. Hakim, M. Noori, M. Cheraghalikhani, A. Bahri, M. Yazdanpanah, I. Ben Ayed, and C. Desrosiers. Nc-ttt: A noise contrastive approach for test-time training. In *Proceedings of the IEEE/CVF Conference on Computer Vision and Pattern Recognition*, pages 6078–6086, 2024.
- A. Radford, J. Wu, R. Child, D. Luan, D. Amodei, I. Sutskever, et al. Language models are unsupervised multitask learners. *OpenAI blog*, 2019.
- M. Riviere, S. Pathak, P. G. Sessa, C. Hardin, S. Bhupatiraju, L. Hussenot, T. Mesnard, B. Shahriari, A. Ramé, J. Ferret, P. Liu, P. Tafti, A. Friesen, M. Casbon, S. Ramos, R. Kumar, L. Lan, et al. Gemma 2: Improving open language models at a practical size. *arXiv preprint arXiv:2408.00118*, 2024.
- J. Schneider. Generative to agentic ai: Survey, conceptualization, and challenges. *arXiv preprint arXiv:2504.18875*, 2025.
- J. Schneider and M. Vlachos. Reflective-net: Learning from explanations. *Data Mining and Knowledge Discovery*, 38(5):2975–2996, 2024.
- R. R. Selvaraju, M. Cogswell, A. Das, R. Vedantam, D. Parikh, and D. Batra. Grad-cam: Visual explanations from deep networks via gradient-based localization. In *Proceedings of the IEEE international conference on computer vision*, pages 618–626, 2017.
- K. Simonyan and A. Zisserman. Very deep convolutional networks for large-scale image recognition. pages 1–14, 2014.
- Y. Sun, X. Wang, Z. Liu, J. Miller, A. Efros, and M. Hardt. Test-time training with self-supervision for generalization under distribution shifts. In *International conference on machine learning*, pages 9229–9248. PMLR, 2020.
- Y. Sun, X. Li, K. Dalal, J. Xu, A. Vikram, G. Zhang, Y. Dubois, X. Chen, X. Wang, S. Koyejo, et al. Learning to (learn at test time): Rnns with expressive hidden states. *arXiv preprint arXiv:2407.04620*, 2024.
- H. Touvron, T. Lavril, G. Izacard, X. Martinet, M.-A. Lachaux, T. Lacroix, B. Rozière, N. Goyal, E. Hambro, F. Azhar, A. Rodriguez, A. Joulin, E. Grave, and G. Lample. The llama 3 herd of models. *arXiv preprint arXiv:2407.21783*, 2024. URL <https://arxiv.org/abs/2407.21783>.
- D. Wang, E. Shelhamer, S. Liu, B. Olshausen, and T. Darrell. Tent: Fully test-time adaptation by entropy minimization. *arXiv preprint arXiv:2006.10726*, 2020.
- S. Wang, D. Zhang, Z. Yan, J. Zhang, and R. Li. Feature alignment and uniformity for test time adaptation. In *Proceedings of the IEEE/CVF Conference on Computer Vision and Pattern Recognition*, pages 20050–20060, 2023.
- Wikipedia. Simple english wikipedia. <https://dumps.wikimedia.org/simplewiki/latest/simplewiki-latest-pages-articles.xml.bz2>, 2024. Accessed: 2024-08.
- C. Zhang, S. Bengio, M. Hardt, B. Recht, and O. Vinyals. Understanding deep learning (still) requires rethinking generalization. *Communications of the ACM*, 64(3):107–115, 2021.
- T. Zhong, Z. Liu, Y. Pan, Y. Zhang, Y. Zhou, S. Liang, Z. Wu, Y. Lyu, P. Shu, X. Yu, et al. Evaluation of openai o1: Opportunities and challenges of agi. *arXiv preprint arXiv:2409.18486*, 2024.

A Appendix

A.1 More related work

(Self-)reflection Our technique bears similarity with reflective techniques that often do not yield a decision based on a single forward pass. Reasoning models like ChatGPT o1 and o3 also perform multiple queries to the same model to obtain answers [Zhong et al., 2024] often involving reflection [Schneider, 2025]. For example, self-refine[Madaan et al., 2024] refines outputs by leveraging uncertainty in the initial answer. The model evaluates its own answer for plausibility and consistency and refines it. There are many more reflective variants. In contrast, we work on a token level, i.e., reflecting on each token rather than a sequence of tokens, using direct uncertainty estimates of the model changing also a model’s parameters. There are also works in the image domain. For example, Schneider and Vlachos [2024] computed explanations for a decision (similar to GradCAM Selvaraju et al. [2017]) and (self-)trained the model on its own explanations. Thus, a decision can either be made using a single forward pass, or using multiple passes (including an explanation). However,

A.2 Qualitative Evaluation using XAI

To illustrate our technique and its impact on the model, i.e., the differences between the baseline model f and its fine-tuned version f_{Opt} , we employed a standard explainability technique called GradCAM[Selvaraju et al., 2017]. A GradCAM visualization highlights areas that are relevant to the predicted class with respect to a specific layer, i.e., we used the 2nd layer of our VGG-16 trained on EMNIST. It relies on products of activation maps and gradients. We wanted to understand the impact on outputs depending on whether the fine-tuning changed the output. We picked one example for each of the following cases: wr2co (Prediction of f wrong, while f_{Opt} ’s is correct), wr2wr, co2wr, co2co. Each of them is shown in a row in Figure 8. The first column shows the image to classify and its label. The 2nd, 4th, and 6h column show GradCAM visualization of the original model f , for the predicted class $m(1)$, the second-most likely class $m(2)$ and for both (i.e., for iFo). Columns 3, 5 and 7 (named $\Delta GradC$) shows the addition of the differences between the GradCAM on f and our optimized model f_{Opt} .² We observe that oftentimes the impact of our method is small, e.g., there are no visible differences and the fine-tuning seems to have little effect. This holds in particular for cases, where the prediction did not change. This can happen due to multiple scenarios, e.g., when the two most likely classes do not rely very much on features shared between both, so that amplifying their relevance as done by iFo might have limited impact. If predictions change due to fine-tuning, the impact is generally also visually more profound as shown in rows 3 and 4 in Figure 8. Note, also that changes happen to both classes, e.g., for wr2co the changes ($\Delta GradC$ columns) are well visible for both classes. Both classes (not just the correct) show stronger emphasis on various regions. For co2wr, also both classes change.

A.3 Datasets and training of classifiers

A.4 More details on experimental setup

Hardware and Software. All experiments were conducted on an Ubuntu 22.04 system equipped with Python 3.12, PyTorch 2.5, CUDA 12.5, and an NVIDIA 4090 RTX GPU. We leveraged torchvision v0.15 for the pre-trained ImageNet models (IMAGENET1KV2 if available otherwise IMAGENET1KV1). The experiments ran for about 2-3 months.

Datasets and Models. References for datasets and models: For image classification, we use ImageNet [Deng et al., 2009], CalTech-256 (Cal256)Griffin et al. [2007], CIFAR-100 (Ci100) [Krizhevsky and Hinton, 2009], and (balanced) EMNIST [Cohen et al., 2017]. We trained VGG-13(V13) [Simonyan and Zisserman, 2014], ResNet-18(R18) [He et al., 2016], and MobileNetV3-13 (M13) [Howard et al., 2019]. For language modeling, we use (from HuggingFace) GPT-2 [Radford et al., 2019] 124MB (version), Llama 3.2 1B [Touvron et al., 2024], QWEN 2.5 1.5B [Chen et al., 2024], and Gemma-2 2B [Riviere et al., 2024]. We evaluate on OpenWebText and open-source replication of the WebText dataset from OpenAI [Gokaslan and Cohen] and SimpleWiki, a collection Wikipedia articles written in simple English [Wikipedia, 2024], and legal contracts [del

²We found this easier to grasp than showing raw differences.

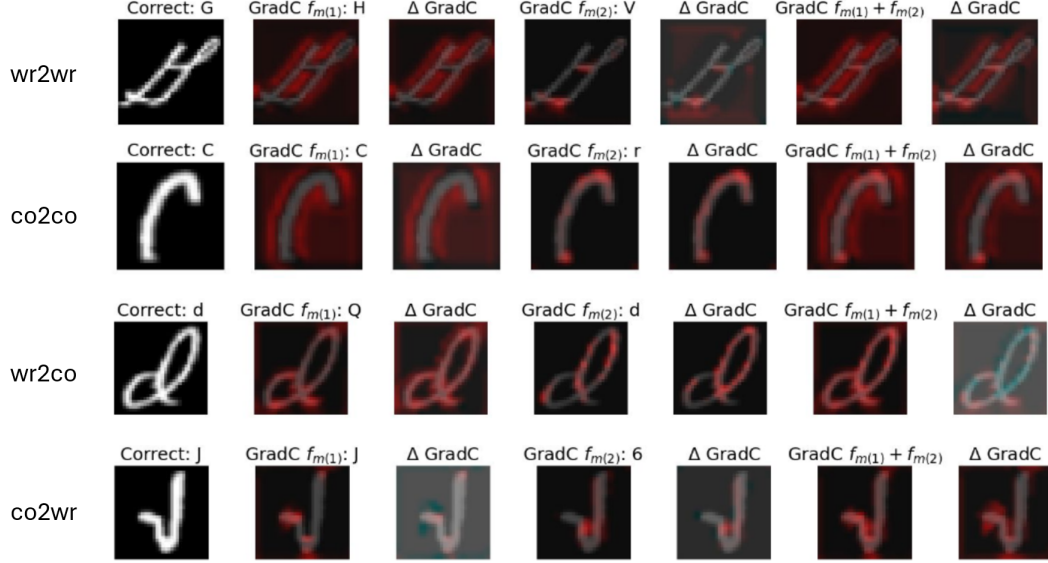


Figure 8: GradCAM visualizations showing changes after optimization ($\Delta GradC$) for different classes $m(1)$, $m(2)$ and both jointly.

Moral].

For pretrained ImageNet networks, we relied on the standard validation data of 50000 samples. For Ci100 and EMNIST we obtained training and test data through random sampling as follows: We joined the pre-defined training and test data into one big dataset and sampled 20000 datapoints (out of 6000) for Ci100, 100000 (out of 131600) for balanced EMNIST, and 10000 (out of 31000) for Cal256. EMNIST images are scaled to 32×32 pixels, and we use standard train/validation splits for all datasets. We used IMAGENET1KV2 versions if available otherwise IMAGENET1KV1. For text-data we used only pre-trained models and, thus, we did not perform any train/test split. Like for any public dataset, we cannot exclude that the models were not already trained on the data. However, one reason for using up to 2B models was that they were far from perfect on this data. Therefore, the fact that the data might have been used for training is not a key concern. The number of samples evaluated for the language models was constrained by our computational resources, i.e., we ran as long as we could. We focused, in particular on the case of iFo as it seemed more promising after evaluating on image data.

Network architectures Our network architectures are given separately.

Training. We conducted one run for ImageNet data and five for each of our self-trained classifier/dataset combination. For training our classifiers on image data, data augmentation consisted of horizontal flipping (except for EMNIST) and shifting randomly by 1 or 2 pixels horizontally or vertically. We used SGD with momentum 0.9 and batchsize 256. We trained for 150 epochs using warm-up and cosine annealing starting from a learning rate of 0.2 and weight decay of 0.0005 across all benchmarks. More details can be found in the supplied code.

A.5 Results

A.6 Additional Plots

A.7 Optimizing softmax outputs instead of logits

Using logs of softmax outputs:

$$\textbf{Given: } \mathbf{z} = (z_1, z_2, \dots, z_K), \quad p_i = \frac{e^{z_i}}{\sum_{j=1}^K e^{z_j}}, \quad \mathbf{y} = (y_1, y_2, \dots, y_K) \text{ with } y_c = 1 \text{ and } y_i = 0 \text{ for } i \neq c.$$

Table 2: Performance for doFo with the same default hyperparameters across all configurations O_{Img}

Dataset	Model	$\frac{ D_{te,1,2} }{ D }$	$ D_{te,1,2} $	Acc. f (Baseline)	Acc. f_{Opt} (Ours, doFo)	Δ_{Acc}
Cal25	M13	17.9	1789	8.82	9.14	0.32
Cal25	R18	27.1	2705	12.26	12.33	0.07
Cal25	V16	11.9	1186	9.07	9.51	0.44
Ci100	M13	4.8	953	19.65	21.1	1.45
Ci100	R18	10.5	2100	23.47	23.72	0.25
Ci100	V16	4.9	986	18.62	20.18	1.56
EMNIS	M13	0.5	463	40.96	40.4	-0.56
EMNIS	R18	0.6	593	39.53	40.07	0.54
EMNIS	V16	0.4	392	38.08	41.14	3.06
ImgNe	CoNeTB	2.6	1280	30.47	32.89	2.42
ImgNe	EffB0	4.8	2403	27.22	27.3	0.08
ImgNe	EffB7	3.5	1730	23.24	23.18	-0.06
ImgNe	MOBV3	3.5	1760	23.86	23.58	-0.28
ImgNe	R50	3.8	1911	27.37	27.84	0.47
ImgNe	VGG16	4.8	2389	23.78	23.65	-0.13

Table 3: Performance for iFo with network dependent learning rate (lr) across all configurations O_{Text}

Dataset	Model	$\frac{ D_{te,1,2} }{ D }$	$ D_{te,1,2} $	lr	Acc. f (Baseline)	Acc. f_{Opt} (Ours, iFo)	Δ_{Acc}
contract	gpt2	21.4	70106	4.03e-02	14.49	15.67	1.18
openwebtext	gpt2	31.2	70094	4.03e-02	11.94	12.29	0.35
simplewiki	gpt2	32.2	70052	4.03e-02	11.49	11.75	0.26
contract	Llama-3.2-1B	8.1	270140	2.29e-03	16.06	16.31	0.25
openwebtext	Llama-3.2-1B	16.3	270248	2.29e-03	13.56	13.67	0.11
simplewiki	Llama-3.2-1B	13.2	270232	2.29e-03	13.53	13.64	0.11
contract	gemma-2-2b	4.5	270111	4.03e-02	11.39	13.86	2.47
openwebtext	gemma-2-2b	7.7	270140	4.03e-02	10.36	12.53	2.17
simplewiki	gemma-2-2b	6.7	270123	4.03e-02	13.04	13.5	0.46
contract	Qwen2.5-1.5B	6.0	260128	1.55e-02	17.45	17.57	0.12
openwebtext	Qwen2.5-1.5B	15.7	270237	1.55e-02	13.42	13.58	0.16
simplewiki	Qwen2.5-1.5B	12.7	260130	1.55e-02	13.02	13.2	0.18

Cross-entropy loss:
$$L = - \sum_{i=1}^K y_i \log p_i = - \log p_c = - \log \left(\frac{e^{z_c}}{\sum_{j=1}^K e^{z_j}} \right).$$

Simplifying:
$$- \log \left(\frac{e^{z_c}}{\sum_{j=1}^K e^{z_j}} \right) = - [\log(e^{z_c}) - \log(\sum_{j=1}^K e^{z_j})] = \log(\sum_{j=1}^K e^{z_j}) - z_c.$$

$$L = \log \left(\sum_{j=1}^K e^{z_j} \right) - z_c.$$

Assuming we have C classes to optimize towards 1 this yields:

$$L = 1/|C| \sum_{c \in C} (\log(\sum_{j=1}^K e^{z_j}) - z_c) = \log(\sum_{j=1}^K e^{z_j}) - 1/|C| \sum_{c \in C} z_c.$$

That is we push each z_j not in C towards minus ∞ , while pushing the others towards positive ∞ .

Assuming we have C classes to optimize towards 0 this yields:

$$L = 1/|C| \sum_{c \in C} z_c - 1/|C| \sum_{c \in C} (\log(\sum_{j=1}^K e^{z_j}) - z_c) = \log(\sum_{j=1}^K e^{z_j}).$$

That is we push each z_j towards minus ∞ , while pushing the others towards positive ∞ .

Thus, comparing optimizing raw logits vs softmax outputs, we see that raw logits allow to focus more directly only on the intended classes by altering their outputs, while softmax impacts directly all class outputs. That is, for our decrement doFo approach we tend to increase the other classes, while for the increment approach iFo, we decrease others. In that sense, softmax yield a combined approach.

Table 4: Performance for doFo with network dependent learning rate (lr) across all configurations
 O_{Text}

Dataset	Model	$\frac{ D_{te,1,2} }{ D }$	$ D_{te,1,2} $	lr	Acc.f (Baseline)	Acc.f _{Opt} (Ours, doFo)	Δ_{Acc}
contract	Qwen2.5-1.5B	6.0	70052	7.43e-06	17.63	17.66	0.03
openwebtext	Qwen2.5-1.5B	15.7	70054	7.43e-06	13.37	13.41	0.04
simplewiki	Qwen2.5-1.5B	12.7	70029	7.43e-06	13.01	13.02	0.01
contract	gemma-2-2b	4.6	90047	1.31e-04	11.54	11.6	0.06
openwebtext	gemma-2-2b	7.7	110036	1.31e-04	10.49	10.55	0.06
simplewiki	gemma-2-2b	6.7	110053	1.31e-04	13.24	13.26	0.02
contract	gpt2	21.4	80115	6.25e-08	14.58	14.63	0.05
openwebtext	gpt2	31.2	70094	6.25e-08	11.94	12.06	0.12
simplewiki	gpt2	32.2	70052	6.25e-08	11.49	11.49	0.0
contract	Llama-3.2-1B	8.0	70031	7.43e-06	16.14	16.17	0.03
openwebtext	Llama-3.2-1B	16.3	70078	7.43e-06	13.38	13.54	0.16
simplewiki	Llama-3.2-1B	13.3	70026	7.43e-06	13.78	13.83	0.05

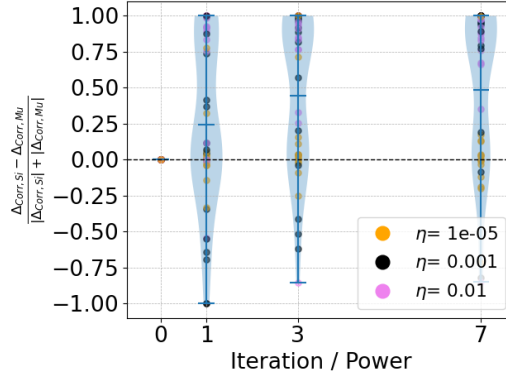


Figure 9: Relative change in predictions Δ_{Corr} over iterations compared to single step with learning rate 2^{Iter} for doFo across all image classifiers, datasets

A.8 Theoretical Motivation with details

Model: We focus on a simple case with three output classes $C = \{y_0, y_1, y_2\}$ and focus classes $F = \{y_0, y_1\}$. To compute the final output y_i being logits we have four input features $X = \{x_0, x_1, x_2, x_3\}$. The input features x_j can be seen as originating from a prior layer l , i.e., $x_j = l(a_j, c'_k) = l(z_i)$. We assume that the optimization process has yield some parameters c_i , which define our network f . Outputs $y_i := f_i(X)$ are computed as:

$$y_0 = c_0x_0 + c_4x_3 \quad (4)$$

$$y_1 = c_1x_1 + c_5x_3 \quad (5)$$

$$y_2 = c_2x_2 + c_6x_3 \quad (6)$$

We apply the intuitive notion that a feature value cannot be negative, i.e., $x_i \geq 0$, which happens, for example, after layer activations pass through a non-linearity like *ReLU*. The model implicitly expresses that the presence of input features $\{x_0, x_1, x_2\}$ is only indicative of class i , i.e., a change of x_i alters only y_i for $i \in \{0, 1, 2\}$. In turn, $c_0 > 0, c_1 > 0, c_2 > 0$. The shared feature x_3 impacts all outputs y_i . It might also be contrastive, i.e., it can be that $c_4 < 0, c_5 < 0, c_6 < 0$. Depending on the sign of c_4, c_5 and c_6 it increases or decreases y_i . Say $x_j = l(a_j, c'_k) = l(z_i)$, i.e., $z_i := (a_j, c'_k)$, is the output of a layer l depending on activations a_j and parameters c'_k . To facilitate our analysis, we assume that x_j are independent, i.e., rely on different parameters and activations. We model dependence using shared parameters and activations through x_3 .

We consider updates to parameters c_i depending on the loss from our methods iFo $L_{iFo} = -(y_0 + y_1)$ (Eq. 2), doFo $L_{doFo} = y_2$ (Eq. 2) and from optimizing just a single class either increasing $L_{y_i,+} = y_i$ or decreasing it $L_{y_i,-} = -y_i$. In short, $L_{y_i,\pm} = \pm y_i$. Note, that for maximizing a class output y_i , the loss is $L_{y_i,-} = -y_i$. We have that $L_{iFo} = -(y_0 + y_1) = L_{y_0,-} + L_{y_1,-}$ and, analogously, $L_{doFo} = y_2 = L_{y_2,+}$.

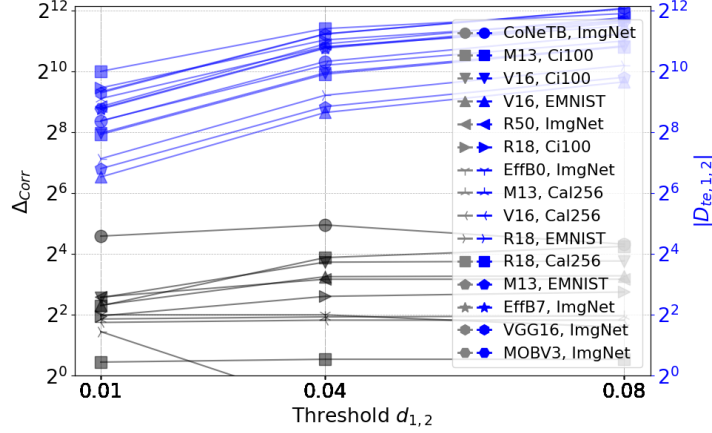


Figure 10: Relation between number of predictions $|D_{te,1,2}|$ and gain in terms in correct predictions Δ_{Corr} due to doFo for image recognition

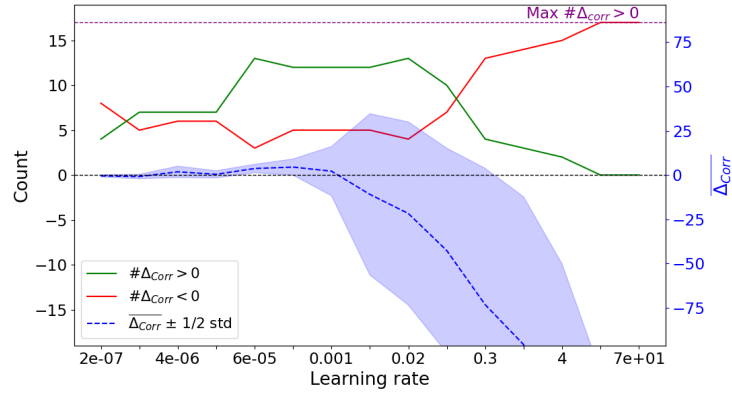


Figure 11: Average Δ_{Corr} and $\#\Delta_{Corr} > 0$ using different learning rates for doFo all image configurations O_{img}

We investigate updates to parameters c_i due to backpropagation:

$$c_i \leftarrow c_i - \eta \frac{\partial L}{\partial c_i} \quad (7)$$

with $L \in \{L_{iFo}, L_{doFo}, L_{y_i, \pm}\}$

Analysis Let us compute updates to c_i . We need the following partial derivatives:

$$\frac{\partial L_{y_j, \pm}}{\partial c_i} = \begin{cases} \pm x_j, & \text{if } i = j \\ \pm x_3, & \text{if } i = 4 + j \\ 0, & \text{otherwise} \end{cases} \quad (8)$$

$$\frac{\partial L_{iFo}}{\partial c_i} = \begin{cases} -x_j, & \text{if } i = j, j \in \{0, 1\} \\ -x_3, & \text{if } i = j, j \in \{4, 5\} \\ 0, & \text{otherwise} \end{cases} \quad (9)$$

$$\frac{\partial L_{doFo}}{\partial c_i} = \begin{cases} x_2, & \text{if } i = 2 \\ x_3, & \text{if } i = 6 \\ 0, & \text{otherwise} \end{cases} \quad (10)$$

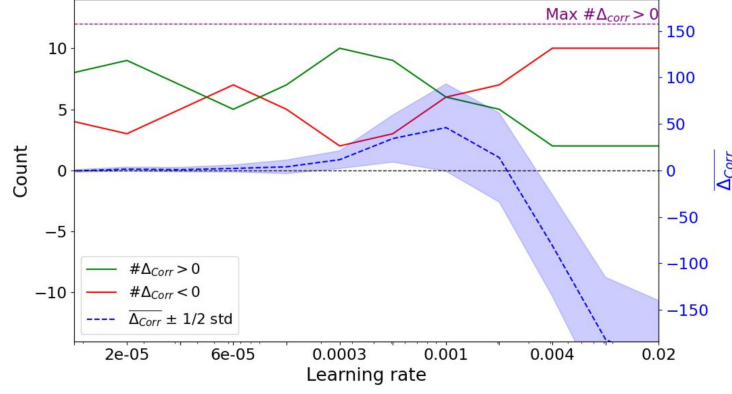


Figure 12: Average Δ_{Corr} using different learning rates for iFo on all text configurations O_{text}

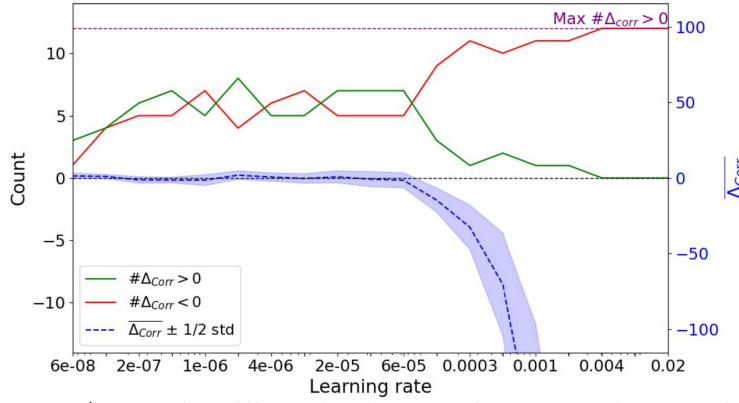


Figure 13: Average Δ_{Corr} using different learning rates for doFo on all text configurations O_{text}

Partial derivatives with respect to z_i :

$$\frac{\partial L_{y_j, \pm}}{\partial z_i} = \pm \left(c_j \frac{\partial x_j}{\partial z_i} + c_{4+j} \frac{\partial x_3}{\partial z_i} \right) \quad (11)$$

$$\frac{\partial L_{iFo}}{\partial z_i} = -c_0 \frac{\partial x_0}{\partial z_i} - c_1 \frac{\partial x_1}{\partial z_i} - (c_4 + c_5) \frac{\partial x_3}{\partial z_i} \quad (12)$$

$$\frac{\partial L_{doFo}}{\partial z_i} = c_2 \frac{\partial x_2}{\partial z_i} + c_6 \frac{\partial x_3}{\partial z_i} \quad (13)$$

Let us compare the updates for loss L_{iFo} using the focus classes y_0 and y_1 and using just either y_0 or y_1 , i.e., the loss $L_{y_0, -}$ or $L_{y_1, -}$. Wlog., we use $L_{y_0, -}$.

The changes related to parameters $\{c_0, c_1\}$ tied to a class-specific feature are identical, e.g., $\frac{\partial L_{iFo}}{\partial c_0} = \frac{\partial L_{y_0, -}}{\partial c_0}$. However, the behavior for the shared feature x_3 differs between iFo and single class optimization. The feature’s impact on outputs can grow or diminish disproportionately: Say both c_4, c_5 have the same sign. Assume $c_4 > 0, c_5 > 0$. Then $\frac{\partial L_{iFo}}{\partial z_i} > \frac{\partial L_{y_0, -}}{\partial z_i}$ as $c_4 + c_5 > c_4$. In turn, the change to the shared feature x_3 is larger. Thus, in the next update also c_4 (and c_5) are changed more strongly than for single class optimization as $\frac{\partial L_{iFo}}{\partial c_i} = x_3$ for $i \in \{4, 5\}$. Thus, there is a “double growth effect,” where the growth of x_3 amplifies the growth of parameters c_4 and c_5 and vice-versa. This can lead to instability in an iterative process, e.g., the shared features becomes the sole decision criteria with exploding coefficients. This “double effect” is not present if we perform just a single step (with large learning rate). However, for both single and multi-step we observe that the shared feature is altered more extremely, potentially, leading to an overreliance on the feature. If both c_4, c_5 have different signs, i.e., the changes to x_3 are less for iFo than for optimizing only y_4 and in turn also c_4, c_5 change less, meaning that the relevance of x_3 to the decision process diminishes relative to single class optimization.

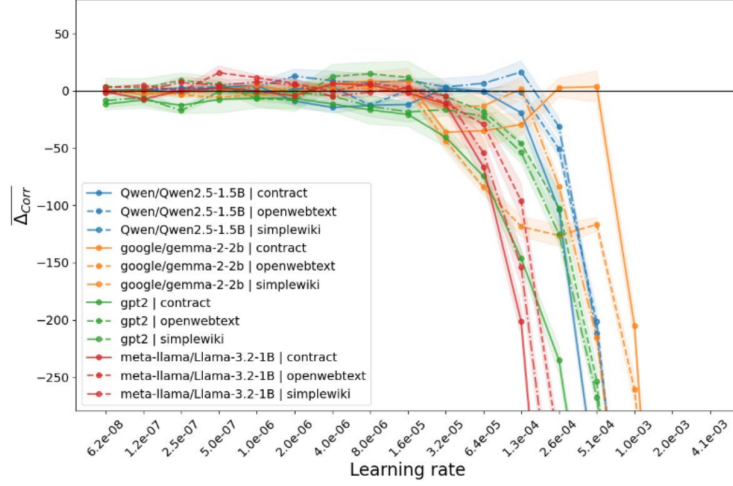


Figure 14: Δ_{Corr} with 1/3 of standard deviation using different learning rates for doFo all text configurations O_{text}

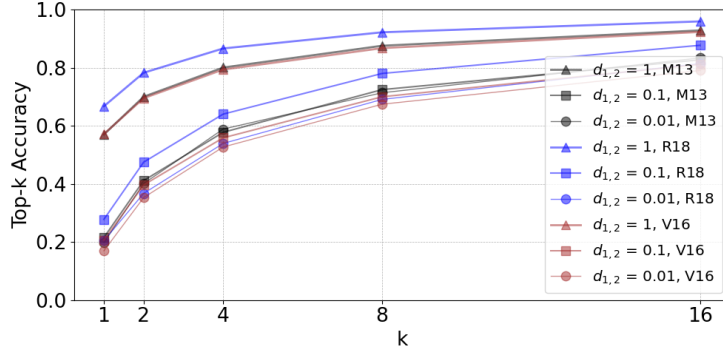


Figure 15: Top-k Accuracy on Cifar-100

Intuitively, if $c_4 \approx c_5$ (both coefficients have the same sign and the same magnitude), i.e., x_3 contributes positively to y_0, y_1 , we make the feature x_3 even more relevant compared to other features. In turn, this diminishes the role of non-shared features. This includes features x_0, x_1 that are only specific to each focus class y_0 and y_1 . It also covers features that are shared with other classes and just one focus class.³ On the one hand relying more on shared features seems flawed as class-specific features that matter only for one of the (focus) classes also play a role in discriminating them. However, the fact that we have high uncertainty and we know that the classifier deemed both classes y_0 and y_1 relevant, justifies that also the shared features play a bigger role as their activation are either relatively large compared to any of the class-specific feature or the class-specific features are of similar magnitude⁴.

Let us compare the updates for loss L_{doFo} with $L_{y_0,-}$. Say c_2, c_3 have the same sign, i.e., feature x_3 increases outputs for all classes or decreases it. Then using $L_{y_0,-}$ increases the relevance of all features c_0 and c_4 , while doFo decreases c_2 and the shared feature x_3 , leading to a stronger reliance of y_0 on features only present y_0 , i.e., x_0 . This behavior is different from iFo, as for iFo x_3 would become more relevant. For, doFo features of out-of-focus classes are deemed irrelevant.

Say $c_4 > 0$ and $c_5 < 0$ (or vice versa), e.g., $c_4 \approx -c_5$. As x_3 decreases for doFo, y_1 grows, while y_0 shrinks. This behavior is also different from iFo, since if $c_4 \approx -c_5$ there is no net impact on c_3 .

³which we did not include in our model for simplicity, but we might as well assume that there exists a y_3 or even y_2 that also depends on x_0 , which would not change any of our computations for iFo and classes y_0, y_1, y_2 .

⁴One might exclude this case by using class-specific features more explicitly to discriminate, e.g., $y_0 = c_0x_0 + c_4x_3 - c_7x_1 - c_8x_2$, which we did not do for readability.

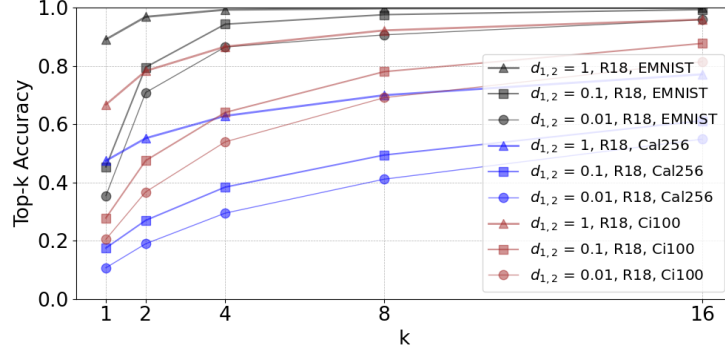


Figure 16: Top-k Accuracy for R18 across datasets

In summary, iFo tends to amplify features that are shared between focus classes F (if their presence contributes positively to the likelihood), while doFo tends to hamper features that are shared between focus and out-of-focus classes.

A.9 Additional experiments and further comments on experiments

Experiment 5 - statistical tests: Many of our plots contain standard deviations providing intuition on the statistical significance of outcomes. Here, we perform a formal analysis based on a simple and conservative model of a fair coin, i.e., each outcome of a configuration is the outcome of a coin toss. If the coin is likely fair, i.e., accuracy gains (coin shows 1 or heads) and losses (coin shows 0 or tails) are both very likely, our methods are not helpful. If it is biased to 1, our methods are helpful. If biased towards 0, our methods make predictions worse. If it is fair, our methods have no impact. For iFo and vision datasets we have that out of 15 configurations 14 yield gains. Assuming it is equally likely to observe gains or no gains, this event would happen with probability:

$$\Pr\{X = 14 \mid p = \frac{1}{2}\} = \binom{15}{14} \left(\frac{1}{2}\right)^{14} \left(\frac{1}{2}\right)^1 = \binom{15}{14} 2^{-15} = \frac{15}{32768} \approx 0.000458.$$

Now, as we picked a learning rate of say 5 options (We have evaluated more than 5 but all learning rates beyond a threshold are clearly non-beneficial), we can assume that we have picked the best outcome out of 5 attempts. This yields:

$$\Pr(\text{at least 1 of 5 sets of 15 throws has exactly 14 ones} \mid p = \frac{1}{2}) = (1 - 2^{-15})^5 - (1 - 16 \cdot 2^{-15})^5 \approx 0.0023.$$

Note, that this is a conservative model as clearly for similar learning, we also observe benefits for most configurations O_{Img} . Thus, modeling a joint outcome would give better results.

Let us consider O_{Text} . Here we pick a learning rate for each of the four models and evaluate on three datasets. Say we pick the best among 5 learning rates for each model. We observe only 1s. How likely is this under a fair coin?

Step 1: Probability of observing three heads (HHH) in one trial

$$q = \left(\frac{1}{2}\right)^3 = \frac{1}{8}$$

Step 2: Probability of at least one HHH in 5 trials (choosing the best result)

$$p = 1 - (1 - q)^5 = 1 - \left(\frac{7}{8}\right)^5 \approx 0.4871$$

Step 3: Probability of repeating this outcome (HHH each time) 4 times

$$P(\text{data} \mid \text{fair coin}) = p^4 \approx 0.4871^4 \approx 0.0563$$

Step 4: Bayesian posterior (assuming equal priors on fair vs. always-heads coin)

$$P(\text{fair} \mid \text{data}) = \frac{0.5 p^4}{0.5 p^4 + 0.5} = \frac{p^4}{1 + p^4} \approx 0.053$$

The fact that gains for both images and text are by chance for iFo is less than 0.0001.

Experiment 6 - Combination with other test-time fine-tuning techniques: Conceptually there is no reason, why our method is in direct conflict with methods using inputs rather than likely predictions for test-time fine-tuning. That is, that one might expect that while their might be some interaction, if both yield gains if applied in isolation, applying them jointly also yields benefits. To provide empirical evidence, we compare against self-supervised learning on the inputs only. That is, for each input X we apply a single optimization step (as for our method) aiming to predict next tokens by using a shifted input of X – as is done for any autoregressive model (see, e.g., code in the NanoGPT repo). We used a learning rate of 1e-3, which is rather large. Smaller learning rates often lead to hard to observe differences. Furthermore, our goal is not to show that optimization on inputs is helpful, but to show that our method is still beneficial given potentially large changes to a model due to fine-tuning on related data. The optimization on inputs only yields an input optimized model f_{In} . This method fine-tuning on a single input sample (i) is closest to ours conceptually and (ii) simple and general. While such an approach is not common for vision, it is related to works for LLMs like Hübötter et al. [2024], Hardt and Sun [2023] that augment inputs based on retrieving additional data. After computing f_{In} , we apply our algorithm 1 on f_{In} . *Results:* Table 5 shows first of all that fine-tuning on inputs does sometimes yield gains sometimes not. However, we applied only one learning rate (we experimented with a lower rate and fewer samples yielding similar outcomes). But as it is not our key concern whether the method is beneficial or not. Rather we want to show that our method remains beneficial despite fine-tuning on the inputs, which is the case for all datasets. The last column in Table 5 shows that if our fine-tuning approach iFo is applied on the model already fine-tuned on inputs, we still observe gains. But it is not clear whether gains are larger or smaller due to the fine-tuning as due to computational limitations, we had to limit the number of samples investigated.

Table 5: Combination of our method *iFo* and fine-tuning on inputs

Model	Dataset	nSamp	Acc. f	Acc. f_{In}	Δ_{Acc}
			(Original model)	(Fine-tuned on Inputs)	(Acc f_{Opt} - Acc. f_{In}) (f_{Opt} = iFo applied on fine-tuned f_{In})
Qwen2.5-1.5B	simplewiki	40012	12.92	12.86	0.32
	contract	40023	17.23	17.18	0.37
	openwebtext	40011	13.84	13.93	0.11
gpt2	contract	40063	15.27	15.43	0.97
	openwebtext	40036	12.65	12.67	0.33
	simplewiki	40029	11.98	11.96	0.21
Llama-3.2-1B	openwebtext	40040	13.48	13.62	0.09
	contract	40012	15.86	16.02	0.17
	simplewiki	40028	13.47	13.45	0.04
gemma-2-2b	contract	30009	11.69	12.55	1.62
	openwebtext	30012	11.05	11.44	1.39
	simplewiki	30023	13.49	13.85	0.02

NeurIPS Paper Checklist

1. Claims

Question: Do the main claims made in the abstract and introduction accurately reflect the paper’s contributions and scope?

Answer: [Yes]

Justification: All key points in the introduction are present in other sections such as experiments and results (4), theory (3 and discussion (6).

2. Limitations

Question: Does the paper discuss the limitations of the work performed by the authors?

Answer: [Yes]

Justification: See section (6).

3. Theory assumptions and proofs

Question: For each theoretical result, does the paper provide the full set of assumptions and a complete (and correct) proof?

Answer: [Yes]

Justification: We have a theory section (3) but we provide no formal proofs but describe a simple model with all calculations to derive conclusions and gain intuition.

4. Experimental result reproducibility

Question: Does the paper fully disclose all the information needed to reproduce the main experimental results of the paper to the extent that it affects the main claims and/or conclusions of the paper (regardless of whether the code and data are provided or not)?

Answer: [Yes]

Justification: The method is simple and with hyperparameters provided (see Algorithm 1). Code is given to reproduce results qualitatively. However, there is no repo that simply allows to run code and produces the exact tables as in the paper. We plan to release a repo later.

5. Open access to data and code

Question: Does the paper provide open access to the data and code, with sufficient instructions to faithfully reproduce the main experimental results, as described in supplemental material?

Answer: [No]

Justification: We plan to release a repo later. Furthermore, the datasets are public and pseudocode is given.

6. Experimental setting/details

Question: Does the paper specify all the training and test details (e.g., data splits, hyperparameters, how they were chosen, type of optimizer, etc.) necessary to understand the results?

Answer: [Yes]

Justification: See section 4 in main part and A.4 in Appendix

7. Experiment statistical significance

Question: Does the paper report error bars suitably and correctly defined or other appropriate information about the statistical significance of the experiments?

Answer: [Yes]

Justification: For key results (performance gains) we also have plots with a notion of variation, e.g., see multiple figures in main part and appendix.

8. Experiments compute resources

Question: For each experiment, does the paper provide sufficient information on the computer resources (type of compute workers, memory, time of execution) needed to reproduce the experiments?

Answer: [Yes]

Justification: See section 4 in main part and A.4 in Appendix

9. Code of ethics

Question: Does the research conducted in the paper conform, in every respect, with the NeurIPS Code of Ethics <https://neurips.cc/public/EthicsGuidelines?>

Answer: [Yes]

Justification: We have reviewed the URL, our work aims at better understanding deep learning and improving performance. There are neither "Potential Harms Caused by the Research Process" nor a "Potential Harmful Consequences".

10. Broader impacts

Question: Does the paper discuss both potential positive societal impacts and negative societal impacts of the work performed?

Answer: [NA]

Justification: NA

11. Safeguards

Question: Does the paper describe safeguards that have been put in place for responsible release of data or models that have a high risk for misuse (e.g., pretrained language models, image generators, or scraped datasets)?

Answer: [NA]

Justification: NA

12. Licenses for existing assets

Question: Are the creators or original owners of assets (e.g., code, data, models), used in the paper, properly credited and are the license and terms of use explicitly mentioned and properly respected?

Answer: [Yes]

Justification: NA

Guidelines: Our datasets and models are all public and cited. Asset /Licenses are: ImageNet (Free for non-commercial research use), Caltech-256 (No explicit license specified), CIFAR-100 (Apache License 2.0), EMNIST (Creative Commons Attribution 4.0 License), OpenWebText (No explicit license specified), SimpleWiki (Creative Commons Attribution-ShareAlike 3.0 Unported License), VGG-13 (CC0 Public Domain), ResNet-18 (BSD 3-Clause License), MobileNetV3 (BSD 3-Clause License), EfficientNet B0/B7 (Apache License 2.0), ResNet-50 (BSD 3-Clause License), ConvNeXt-Base (MIT License), VGG-16 BN (BSD 3-Clause License), GPT-2 (MIT License), Llama 3.2 1B (Llama 3.2 Community License Agreement), QWEN 2.5 1.5B (Apache License 2.0), Gemma-2 2B (Apache License 2.0)

13. New assets

Question: Are new assets introduced in the paper well documented and is the documentation provided alongside the assets?

Answer: [NA]

Justification: NA

14. Crowdsourcing and research with human subjects

Question: For crowdsourcing experiments and research with human subjects, does the paper include the full text of instructions given to participants and screenshots, if applicable, as well as details about compensation (if any)?

Answer: [NA]

Justification: NA

15. Institutional review board (IRB) approvals or equivalent for research with human subjects

Question: Does the paper describe potential risks incurred by study participants, whether such risks were disclosed to the subjects, and whether Institutional Review Board (IRB) approvals (or an equivalent approval/review based on the requirements of your country or institution) were obtained?

Answer: [NA]

Justification: NA

16. Declaration of LLM usage

Question: Does the paper describe the usage of LLMs if it is an important, original, or non-standard component of the core methods in this research? Note that if the LLM is used only for writing, editing, or formatting purposes and does not impact the core methodology, scientific rigorousness, or originality of the research, declaration is not required.

Answer: [NA]

Justification: NA